

# Cu<sup>(I)</sup>(2,9-Bis(trifluoromethyl)-1,10-phenanthroline)<sub>2</sub><sup>+</sup> Complexes: Correlation between Solid-State Structure and Photoluminescent Properties

Andrey Yu. Kovalevsky,\* Milan Gembicky, and Philip Coppens\*

Chemistry Department, University at Buffalo, State University of New York, Buffalo, New York 14260

Received March 18, 2004

The 90 K solid-state structures, room temperature absorption, and room temperature and 17 K emission spectra of seven different salts of [Cu(I)(bfp)<sub>2</sub>]<sup>+</sup> (bfp = 2,9-bis(trifluoromethyl)-1,10-phenanthroline) have been determined. To quantify the distortion of the Cu coordination environment, a distortion parameter  $\zeta$  is defined that is a combined measure of the flattening, rocking, and wagging distortions of the complex cations. In general, the distortion in the (bfp) cations is less than found previously for Cu(I)(dmp)<sub>2</sub> (dmp = 2,9-dimethyl-1,10-phenanthroline) salts, in particular the flattening is reduced because of the bulkier 2,9-substituents. The 17 K lifetimes range up to 1.8  $\mu$ s in the series of solids examined and, with the marked exception of the BF<sub>4</sub><sup>-</sup> salt, correlate linearly with the distortion parameter  $\zeta$ . The emission wavelength red-shifts with decreasing lifetime, which implies that an increased ground-state distortion is associated with a smaller energy gap.

## Introduction

Photoluminescent copper(I) complexes are viewed as a favorable alternative to the polypyridine Ru(II) compounds<sup>1</sup> that have been extensively utilized in molecular solar energy conversion devices<sup>2</sup> and for molecular sensing.<sup>3</sup> Copper compounds, in general, are reasonably inexpensive and environmentally benign compared to their ruthenium analogues. To be used as energy conversion or sensing materials, the Cu(I) systems have to possess strong absorption and emission in the visible region of the spectrum and appropriate redox properties.<sup>4</sup>

In 1980, Blaskie and McMillin discovered the long lifetime emission of the Cu<sup>(I)</sup>(diimine)<sub>2</sub><sup>+</sup> (diimine = substituted 1,10-phenanthroline) systems.<sup>5</sup> Cu(dmp)<sub>2</sub><sup>+</sup> complexes (dmp = 2,9-

dimethyl-1,10-phenanthroline) were found to have strong absorption around 450 nm and weak emission in the red ( $\approx$ 730 nm in CHCl<sub>3</sub> at room temperature) due to population of a <sup>3</sup>MLCT state. By replacing the methyl groups in positions 2 and 9 of the phenanthroline with bulkier substituents the energy, the intensity of the emission and the excited state lifetime are dramatically affected.<sup>6,7</sup> For instance, the lifetime of the excited triplet state of Cu(dmp)<sub>2</sub><sup>+</sup> in a glass matrix at 77 K was measured as 570 ns. Substitution of the methyl group by a butyl group to give Cu(dbp)<sub>2</sub><sup>+</sup> (dbp = 2,9-dibutyl-1,10-phenanthroline) produced a 3-fold increase of the lifetime to 1.8  $\mu$ s, whereas the emission maximum blue-shifted from 730 to 665 nm with an intensity enhancement of almost an order of magnitude ( $\phi = 0.062$  for Cu(dmp)<sub>2</sub><sup>+</sup>,  $\phi = 0.40$  for Cu(dbp)<sub>2</sub><sup>+</sup>).<sup>8</sup> Eggleston and co-workers<sup>9</sup> compared a series of bis-phenanthroline copper compounds containing methyl, *n*-butyl, *n*-octyl, neopentyl, and *sec*-butyl substituents at the

\* Author to whom correspondence should be addressed. E-mail: coppens@buffalo.edu.

- (1) Chen, P. Y.; Meyer, T. J. *Chem. Rev.* **1998**, *98*, 1439–1478.
- (2) (a) Islam, A.; Sugihara, H.; Arakawa, H. J. *Photochem. Photobiol.* **2003**, *158*, 131–138. (b) Kelly, C. A.; Meyer, G. J. *Coord. Chem. Rev.* **2001**, *211*, 295–315. (c) Schwarz, O.; van Loyen, D.; Jockusch, S.; Turro, N. J.; Dürr, H. J. *Photochem. Photobiol. A* **2000**, *132*, 91–98.
- (3) (a) Chang-Yen, D. A.; Lvov, Y.; McShane, M. J.; Gale, B. K. *Sens. Actuators, B* **2002**, *B87*, 336–345. (b) Rowe, H. M.; Xu, W.; Demas, J. N.; DeGraff, B. A. *Appl. Spectrosc.* **2002**, *56*, 167–173.
- (4) Bigzotti, C. A.; Argazzi, R.; Kleverlaan, C. J. *Chem. Soc. Rev.* **2000**, *29*, 87–96.
- (5) Blaskie, M. W.; McMillin, D. R. *Inorg. Chem.* **1980**, *19*, 3519–3522.

- (6) Ichinaga, A. K.; Kirchoff, J. R.; McMillin, D. R.; Dietrich-Buchecker, C. O.; Sauvage, J.-P. *Inorg. Chem.* **1987**, *26*, 4290–4292.
- (7) Phifer, C. C.; McMillin, D. R. *Inorg. Chem.* **1986**, *25*, 1329–1333.
- (8) Everly, R. M.; Ziessel, R.; Suffert, J.; McMillin, D. R. *Inorg. Chem.* **1991**, *30*, 559–561.
- (9) (a) Eggleston, M. K.; McMillin, D. R.; Koenig, K. S.; Pallenberg, A. J. *Inorg. Chem.* **1997**, *36*, 172–176. (b) Eggleston, M. K.; Fanwick, P. E.; Pallenberg, A. J.; McMillin, D. R. *Inorg. Chem.* **1997**, *36*, 4007–4010.

2,9-positions and concluded that the flattening distortion upon excitation is increasingly hindered as the size of the substituents increases. This prevents the expansion of the coordination number by axial substitution in solution, thereby extending the lifetime of the excited species. The findings were more recently supported by the studies on 2,9-aryl and alkyl-substituted bis-1,10-phenanthroline copper(I) complexes.<sup>10</sup>

Recently, Miller et al.<sup>11</sup> reported the synthesis and solution spectroscopic properties of a [Cu(bfp)<sub>2</sub>](PF<sub>6</sub>) complex, where bfp = 2,9-bis(trifluoromethyl)-1,10-phenanthroline. The compound has a very strong absorption in the 400–500 nm range ( $\lambda_{\text{max}} = 462 \text{ nm}$ ,  $\epsilon \approx 11000 \text{ M}^{-1} \text{ cm}^{-1}$  in CH<sub>2</sub>Cl<sub>2</sub>) and is highly emissive in dichloromethane at room temperature. The quantum yield of emission ( $\varphi$ ) was determined to be  $3.3 \times 10^{-3}$ , a 14-fold increase compared to [Cu(dmp)<sub>2</sub>](PF<sub>6</sub>)<sup>12</sup> with an excited-state lifetime of the <sup>3</sup>MLCT excited state of 165 ns in deoxygenated CH<sub>2</sub>Cl<sub>2</sub>. Cyclic voltammetry has shown the \*[Cu(bfp)<sub>2</sub>]<sup>+</sup> excited state to have potent photooxidative as well as effective photoreductive properties.

The photochemical properties of the Cu<sup>(I)</sup>diimines in the crystalline solid state are much less explored. Earlier, we reported that the emission from the <sup>3</sup>MLCT excited state of the Cu(dmp)<sub>2</sub><sup>+</sup> cation is very dependent on the geometry and crystalline environment of the cation in different solids.<sup>13</sup> For instance, the 16 K lifetime of the calix[4]arene salt is only 0.3  $\mu\text{s}$ , whereas it is as much as eight times longer for the *p*-tosylate salt ( $\tau = 2.4 \mu\text{s}$  at 16 K). However, no correlation between the ground-state geometry of the copper(I) cation and its photoluminescent properties was evident as the dihedral angle between the two dmp ligands shows a deviation of as much as 17° from the ideal value of 90°. The [Cu(bfp)<sub>2</sub>]<sup>+</sup> salts, on the other hand, provide a better choice since the presence of 12 fluorine atoms in the vicinity of the central metal atom reduces the conformational flexibility and thus provides more similar ground states.

Here we report on the structural and spectroscopic properties of Cu(bfp)<sub>2</sub><sup>+</sup> complexes containing different counterions in the solid state. The correlation between the molecular structure of the cation and its emission properties is also discussed.

## Experimental Section

**Preparation of the Copper(I) Complexes. (a) Starting Materials.** 2,9-Bis(trichloromethyl)-1,10-phenanthroline was prepared by a literature method.<sup>14</sup> SbF<sub>3</sub>, SbF<sub>5</sub>, [Cu(CH<sub>3</sub>CN)<sub>4</sub>](PF<sub>6</sub>), silver tri-

fluoromethanesulfonate (AgOTf), and sodium 9,10-anthraquinone-2-sulfonate (NaAQSO<sub>3</sub>) are commercially available from either Strem or Aldrich and were used without further purification.

**(b) Synthesis of bfp (2,9-Bis(trifluoromethyl)-1,10-phenanthroline).** In a drybox 2,9-bis(trichloromethyl)-1,10-phenanthroline (1 g, 2.41 mmol) and SbF<sub>3</sub> (10 g, 56 mmol) were mixed in a mortar and ground to a fine homogeneous powder. The mixture obtained was transferred to a 50 mL round-bottom flask, and SbF<sub>3</sub> (1 mL, 13.8 mmol) (*Caution: extremely air- and water-sensitive*) was added. The flask was fitted with a condenser and then transferred outside the drybox, keeping the components under inert atmosphere. It was immersed into a preheated (180 °C) oil bath, and during the next 20–25 min, the mixture was melted by heating to 220 °C. After reaching 220 °C, the melt was slowly cooled to room temperature. The resulting solid was treated with water (50 mL  $\times$  3 times) in an ultrasonic bath. The acidity of the water solution was decreased to pH 4 with NaOH (20% in water). It was then extracted with EtOAc (150 mL  $\times$  3 times). The combined organic extracts were dried over anhydrous Na<sub>2</sub>CO<sub>3</sub>, filtered, and evaporated to dryness to give 500 mg (80%) of the crystalline product. The synthetic procedure is superior to the one published by Beer et al.<sup>15</sup> in that the yield is increased from 18% to 80% and no column chromatography is required to obtain the crystalline product.

**(c) [Cu(bfp)<sub>2</sub>](BF<sub>4</sub>) (1) and [Cu(bfp)<sub>2</sub>](PF<sub>6</sub>) (2).** Complexes 1 and 2 were prepared by the method described previously.<sup>11</sup> Crystals were obtained by diethyl ether vapor diffusion into a CH<sub>2</sub>Cl<sub>2</sub> solution of the corresponding copper complex. All procedures described here and below produced crystals suitable for X-ray diffraction analysis.

**(d) [Cu(bfp)<sub>2</sub>](Br·H<sub>2</sub>O) (3).** To a green solution of CuBr<sub>2</sub> (18 mg, 0.079 mmol) in 15 mL of acetone L-ascorbic acid (21 mg, 0.119 mmol) dissolved in 2 mL of water was added in order to reduce the Cu<sup>(II)</sup> species to Cu<sup>(I)</sup>. The bfp ligand (50 mg, 0.158 mmol, dissolved in 2 mL acetonitrile) was then added to the clear colorless solution, and the resulting bright orange solution was stirred for 30 min at room temperature. The solvent was removed in vacuo, and the orange solid was recrystallized from acetone by diethyl ether vapor diffusion to give large orange-red parallelepipeds (~70% yield).

**(e)  $\alpha$ -[Cu(bfp)<sub>2</sub>](OTf) (4) and  $\beta$ -[Cu(bfp)<sub>2</sub>](OTf) (5).** CuCl<sub>2</sub>·H<sub>2</sub>O (13.5 mg, 0.079 mmol) was dissolved in 5 mL of warm (50 °C) water, and AgOTf (41 mg, 0.158 mmol) was added. The AgCl precipitate was then filtered, and L-ascorbic acid (21 mg, 0.119 mmol) was added. To the resulting colorless solution bfp (50 mg, 0.158 mmol, dissolved in 2 mL of acetonitrile) was added, and the bright orange solution was stirred for 30 min. The solvents were removed in vacuo to give a quantitative yield of [Cu(bfp)]OTf. Crystals were obtained by diethyl ether vapor diffusion into an acetone solution for  $\alpha$ -[Cu(bfp)<sub>2</sub>](OTf) (4) and into an acetonitrile solution for  $\beta$ -[Cu(bfp)<sub>2</sub>](OTf) (5).

**(f) [Cu(bfp)<sub>2</sub>](AQSO<sub>3</sub>)<sub>0.75</sub>(BF<sub>4</sub>)<sub>0.25</sub>·0.5H<sub>2</sub>O (6).** Cu(BF<sub>4</sub>)<sub>2</sub>·6H<sub>2</sub>O (19 mg, 0.079 mmol), NaAQSO<sub>3</sub> (40 mg, 0.13 mmol), and L-ascorbic acid (21 mg, 0.119 mmol) were dissolved in 10 mL of hot water (~80 °C), the solution turned light yellow. bfp (50 mg, 0.158 mmol), dissolved in 2 mL of acetonitrile) was added to the solution, which was then stirred for 20 min at 80 °C. After cooling to room temperature, an orange precipitate of 6 was collected on a frit and dried in air (yield 90%). Diethyl ether vapor diffusion into the acetonitrile solution of the product gave large bright red crystals of the mixed salt.

- (10) (a) Miller, M. T.; Gantzel, P. K.; Karpishin, T. B. *Inorg. Chem.* **1999**, *38*, 3414–3422. (b) Cunningham, C. T.; Cunningham, K. L. H.; Michalec, J. F.; McMillin, D. R. *Inorg. Chem.* **1999**, *38*, 4388–4392. (c) Cunningham, C. T.; Moore, J. J.; Cunningham, K. L. H.; Fanwick, P. E.; McMillin, D. R. *Inorg. Chem.* **2000**, *39*, 3638–3644. (d) Miller, M. T.; Gantzel, P. K.; Karpishin, T. B. *J. Am. Chem. Soc.* **1999**, *121*, 4292–4293.
- (11) Miller, M. T.; Gantzel, P. K.; Karpishin, T. B. *Angew. Chem., Int. Ed.* **1998**, *37*, 1556–1558.
- (12) Ruthkosky, M.; Castellano, F. N.; Meyer, G. J. *Inorg. Chem.* **1996**, *35*, 6406–6412.
- (13) Kovalevsky, A. Yu.; Gembicky, M.; Novozhilova, I. V.; Coppens, P. *Inorg. Chem.* **2003**, *42*, 8794–8802.
- (14) Newkome, G. R.; Kiefer, G. E.; Puckett, W. E.; Vreeland, T. J. *Org. Chem.* **1983**, *48*, 5112–5114.

- (15) Beer, R. H.; Jimenez, J.; Drago, R. S. *J. Org. Chem.* **1993**, *58*, 1746–1747.

Table 1. Crystallographic Data for  $[\text{Cu}(\text{bfp})_2]^{+}$  Complexes at 90 K

	BF <sub>4</sub> <sup>-</sup> 1	PF <sub>6</sub> <sup>-</sup> 2	Br·H <sub>2</sub> O 3	OTf α 4	OTf β 5	(AQSO <sub>3</sub> ) <sub>0.75</sub> (BF <sub>4</sub> ) <sub>0.25</sub> ·0.5H <sub>2</sub> O 6	AQSO <sub>3</sub> ·CH <sub>3</sub> CN 7
empirical formula	C <sub>28</sub> H <sub>12</sub> N <sub>4</sub> F <sub>16</sub> BCu	C <sub>28</sub> H <sub>12</sub> N <sub>4</sub> F <sub>18</sub> PCu	C <sub>28</sub> H <sub>14</sub> N <sub>4</sub> O <sub>2</sub> F <sub>12</sub> BrCu	C <sub>29</sub> H <sub>12</sub> N <sub>4</sub> O <sub>3</sub> F <sub>15</sub> SCu	C <sub>29</sub> H <sub>12</sub> N <sub>4</sub> O <sub>3</sub> F <sub>15</sub> SCu	C <sub>38.5</sub> H <sub>18</sub> N <sub>4</sub> O <sub>4.25</sub> F <sub>13.5</sub> B <sub>0.75</sub> Br <sub>0.25</sub> Cu	C <sub>44</sub> H <sub>22</sub> N <sub>4</sub> O <sub>8</sub> F <sub>12</sub> SCu
cryst size (mm)	0.25 × 0.20 × 0.20	0.25 × 0.20 × 0.15	0.10 × 0.10 × 0.05	0.35 × 0.35 × 0.10	0.40 × 0.10 × 0.05	0.20 × 0.15 × 0.08	0.5 × 0.13 × 0.10
cryst syst	orthorhombic	orthorhombic	triclinic	monoclinic	monoclinic	monoclinic	orthorhombic
space group	<i>P</i> 2 <sub>1</sub> 2 <sub>1</sub> 2 <sub>1</sub>	<i>P</i> 2 <sub>1</sub> 2 <sub>1</sub> 2 <sub>1</sub>	<i>P</i> 1	<i>P</i> 2 <sub>1</sub> / <i>c</i>	<i>C</i> 2/ <i>c</i>	<i>P</i> 2 <sub>1</sub> / <i>n</i>	<i>P</i> bca
<i>a</i> (Å)	12.0887(2)	12.3673(2)	8.8520(3)	16.0114(5)	30.328(1)	16.1323(9)	27.0527(9)
<i>b</i> (Å)	13.0935(2)	13.4042(2)	12.4188(4)	14.0099(4)	8.8882(4)	13.5414(8)	10.5537(3)
<i>c</i> (Å)	17.6673(3)	17.7511(3)	13.1541(5)	14.5051(4)	26.681(1)	33.186(2)	28.2487(9)
α (deg)	90	90	73.257(2)	90	90	90	90
β (deg)	90	90	83.336(2)	113.565(1)	124.059(1)	97.876(1)	90
γ (deg)	90	90	89.079(2)	90	90	7181.3(7)	90
<i>V</i> (Å <sup>3</sup> )	2796.44(8)	2942.67(8)	1375.16(8)	2982.4(2)	5958.2(4)	8065.2(4)	8065.2(4)
<i>Z</i>	4	4	2	4	8	8	8
ρ <sub>calc</sub> , cm <sup>-3</sup>	1.859	1.898	1.917	1.882	1.884	1.742	1.687
θ <sub>min</sub> –θ <sub>max</sub>	2.29–28.01	2.24–31.24	1.63–25.01	2.11–34.01	2.43–26.02	1.50–25.03	1.63–25.02
min, max transm	0.803, 0.838	0.799, 0.872	0.798, 0.891	0.735, 0.912	0.705, 0.955	0.861, 0.944	0.719, 0.933
abs correction	SADABS 2.10	SADABS 2.10	SADABS 2.10	SADABS 2.10	SADABS 2.10	SADABS 2.10	SADABS 2.10
reflns collected	39876	53131	13754	63095	39816	67667	73750
unique reflns ( <i>R</i> <sub>int</sub> )	6751 (0.038)	8815 (0.042)	4832 (0.048)	11792 (0.040)	5852 (0.045)	12589 (0.087)	7114 (0.044)
obsd reflns (no. of parameters)	6074 (451)	7300 (464)	3403 (418)	9379 (478)	4952 (478)	8304 (1112)	5685 (615)
<i>R</i> <sub>1</sub> ( <i>F</i> > 4( <i>σ</i> )*), w <i>R</i> <sub>2</sub>	0.035, 0.093	0.045, 0.124	0.044, 0.118	0.033, 0.092	0.032, 0.090	0.092, 0.228	0.038, 0.121
GOF	1.080	1.072	1.032	1.070	1.048	1.144	1.200

(g)  $[\text{Cu}(\text{bfp})_2](\text{AQSO}_3) \cdot \text{CH}_3\text{CN}$  (7). Compound 7 was synthesized by a similar technique as used for the preparation of 6, but starting with  $\text{CuCl}_2 \cdot \text{H}_2\text{O}$  (27 mg, 0.158 mmol),  $\text{NaAQSO}_3$  (98 mg, 0.316 mmol), and  $\text{bfp}$  (100 mg, 0.316 mmol) (yield 90%). Crystals were obtained by the same method as for 6.

**X-ray Crystallography.** X-ray diffraction data on 1–7 were collected at 90(1) K using a Bruker SMART1000 CCD diffractometer installed at a rotating anode source (Mo  $K\alpha$  radiation) and equipped with an Oxford Cryosystems nitrogen gas-flow apparatus. The data were collected by the rotation method with  $0.3^\circ$  frame width ( $\omega$  scan) and 20–40 s exposure time per frame. For each complex, four data sets (600 frames in each set) were collected, nominally covering half of reciprocal space. The data were integrated, scaled, sorted, and averaged using the SMART software package.<sup>16</sup> The structures were solved by direct methods, using SHELXTL NT Version 5.10<sup>17</sup> and refined by full-matrix least squares against  $F^2$ . The displacement parameters of non-hydrogen atoms were refined anisotropically. Hydrogen atoms were located in difference electron density maps and subsequently refined using the “riding” model for aromatic atoms with  $U_{\text{iso}} = 1.2U_{\text{eq}}$  of the connected carbon, except for the  $\text{CH}_3$  and  $\text{H}_2\text{O}$  hydrogens, which were placed in idealized positions with  $U_{\text{iso}} = 1.5U_{\text{eq}}$ .

In complexes 2 and 3, one of the  $\text{CF}_3$  groups is disordered into two positions by a  $60^\circ$  rotation around the  $\text{C}_{\text{Ar}}-\text{C}(\text{F}_3)$  bonds, with the occupancies refining to 60/40% and 63/37%, respectively. In 6, the asymmetric unit contains two  $[\text{Cu}(\text{bfp})_2]^+$  cations, one  $\text{AQSO}_3^-$  anion being located on a fully occupied crystallographic site, whereas the other anionic site is shared by a second  $\text{AQSO}_3^-$  and a  $\text{BF}_4^-$  anion with 50/50% populations. In addition, one of the fluorine atoms of  $\text{BF}_4^-$  is disordered over two equally populated positions. All disordered atoms were refined isotropically.

**UV–Vis Absorption and Photoluminescence Spectroscopy.** UV–Vis absorption experiments were performed on a Perkin–Elmer Lambda 35 UV–Vis spectrometer equipped with an integrating sphere for reflectance spectroscopy. The spectra were collected in the 300–1100 nm range at room temperature. The samples were prepared by grinding the crystals with  $\text{MgO}$  powder, which is used as the inert matrix. Photoluminescence measurements were carried out on a home-assembled emission detection system. Samples ( $\sim 0.5$ – $1$  mm-sized single crystals) were mounted on a copper pin attached to a DISPLEX cryorefrigerator. The metallic vacuum chamber with quartz windows, attached to the cryostat, is evacuated to approximately  $10^{-7}$  bar with a turbo-molecular pump. Samples were cooled to 17 K. The crystals were irradiated with 500 nm light from a pulsed  $\text{N}_2$ -dye laser. The emitted light was collected by an Oriel 77348 PMT device, positioned at  $90^\circ$  to the incident laser beam, and processed by a LeCroy LT372 digital oscilloscope with 4 GHz sampling rate.

## Results and Discussion

**Structure of the  $[\text{Cu}(\text{bfp})_2]^+$  Cation in Different Solids.** Crystallographic and selected structural data for complexes 1–7 are given in Tables 1 and 2, respectively. Final positional, isotropic, and anisotropic displacement parameters together with bond lengths and angles are listed in Tables S1–S28 of the Supporting Information.

In a preceding paper,<sup>13</sup> we demonstrated that the  $\text{Cu}(\text{dmp})_2^+$  cation can adopt a large variety of conformations

(16) SMART and SAINTPLUS—Area Detector Control and Integration Software, version 6.01; Bruker AXS: Madison, WI, 1999.

(17) SHELXTL—An Integrated System for Solving, Refining and Displaying Crystal Structures from Diffraction Data, version 5.10; Bruker AXS: Madison, WI, 1997.

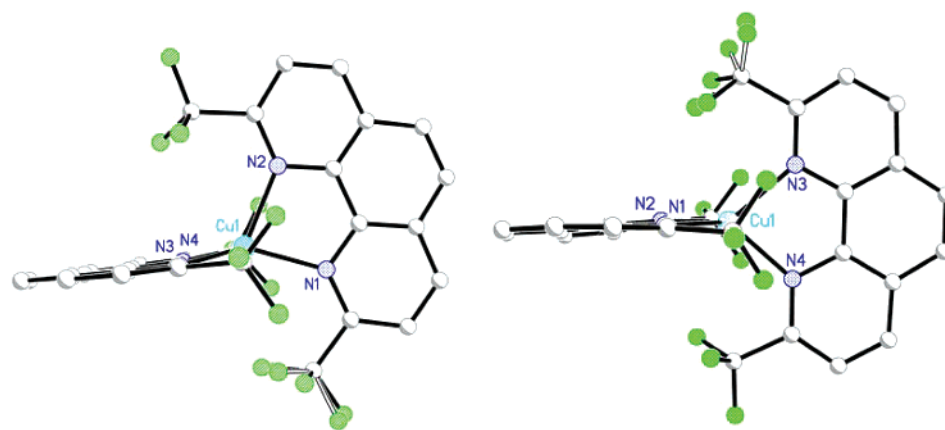


**Figure 1.** Geometry of Cu(bfp)<sub>2</sub><sup>+</sup> cations in complexes **4** (triflate,  $\alpha$ -polymorph) and **3** (bromide). The complexes are drawn in an N–C<sub>Ar</sub>–C<sub>Ar</sub>–N plane.

**Table 2.** Selected Structural Data for [Cu(bfp)<sub>2</sub>]<sup>+</sup> Complexes

	BF <sub>4</sub> <b>1</b>	PF <sub>6</sub> <b>2</b>	Br H <sub>2</sub> O <b>3</b>	( $\alpha$ )OTf	( $\beta$ )OTf <b>5</b>	(AQSO <sub>3</sub> ) <sub>0.75</sub> (BF <sub>4</sub> ) <sub>0.25</sub> 0.5H <sub>2</sub> O <b>6</b>	AQSO <sub>3</sub> CH <sub>3</sub> CN <b>7</b>
Cu1–N1, Å	2.017(2)	2.004(2)	2.034(4)	2.026(1)	2.048(2)	2.034(8), 2.033(7)	2.063(3)
Cu1–N2, Å	2.058(2)	2.060(3)	2.050(4)	2.060(1)	2.046(2)	2.020(7), 2.051(7)	2.021(3)
Cu1–N3, Å	2.068(2)	2.025(2)	2.057(4)	2.054(1)	2.076(2)	1.999(8), 2.004(8)	2.038(3)
Cu1–N4, Å	2.008(2)	2.048(3)	2.031(4)	2.025(1)	2.025(2)	2.053(7), 2.070(7)	2.046(3)
N–Cu–N, °	83.20(9)	83.4(1)	82.7(2)	82.99(4)	82.59(7)	82.7(3), 82.9(3)	82.9(1)
	83.46(9)	83.5(1)	82.7(2)	83.13(4)	82.74(7)	83.6(3), 83.5(3)	83.0(1)
	115.51(8)	115.8(1)	120.9(2)	116.01(4)	117.99(7)	115.6(3), 118.9(3)	115.5(1)
	120.30(9)	117.3(1)	124.5(2)	120.81(4)	120.90(8)	123.9(3), 122.0(3)	123.7(1)
	122.06(9)	125.3(1)	125.5(2)	121.40(4)	128.25(7)	126.4(3), 123.8(3)	127.7(1)
	135.77(9)	134.9(1)	126.3(2)	136.14(4)	129.20(7)	129.2(3), 130.5(3)	128.7(1)
	Distortions around Cu						
$\theta_x$ , °	82.5	85.0	88.8	81.5	89.6	85.6, 85.9	86.0
$\theta_y$ , °	80.5	78.7	88.2	81.6	83.4	83.2, 84.5	83.0
$\theta_z$ , °	87.6	87.5	86.7	87.1	89.6	86.6, 88.8	85.9
$\zeta_{CD}$	<b>0.896</b>	<b>0.899</b>	<b>0.965</b>	<b>0.893</b>	<b>0.959</b>	<b>0.921, 0.941</b>	<b>0.918</b>
Cu displ. from bfp planes (Å)	0.145	0.205	0.038	0.127	0.051	0.003, 0.109	0.021
	0.317	0.211	0.048	0.303	0.059	0.097, 0.142	0.031

in the crystalline phase, with rocking and flattening distortions from 90° as large as 16° and 17°, respectively. In the structures of Cu(bfp)<sub>2</sub><sup>+</sup> complexes, the geometry around the central copper atom shows a much smaller variation than observed for the bis-dmp ions (Table 2, Figure 1). This is attributed to the difference in van der Waals radii of the H and F atoms ( $r_{vdw}(H) = 1.16$  Å,  $r_{vdw}(F) = 1.40$  Å).<sup>18</sup> The presence of bulkier CF<sub>3</sub> groups in the 2- and 9-positions of the 1,10-phenanthroline ligands interferes with any substantial amount of flattening, which would require a decrease of the dihedral angle between the dmp planes.

The distortions around copper can be described by the  $\theta_x$ ,  $\theta_y$ , and  $\theta_z$  angles, as defined by White and co-workers.<sup>19</sup>  $\theta_x$  and  $\theta_y$  describe the “rocking” and “wagging” distortions, respectively; whereas  $\theta_z$  corresponds to the flattening. In the particular case of homoleptic copper(I) complexes, such as described in this paper,  $\theta_x$  and  $\theta_y$  are interchangeable (i.e., rocking and wagging are indistinguishable).

The distortions in complexes **1–7** are compared in Table 2.  $\theta_x$  ranges from 81.5° to 88.8°, while  $\theta_y$  ranges from 78.7°

to 88.2°. As expected flattening is limited in the bfp complexes reported here,  $\theta_z$  varying only from 85.9° to 89.6°. Comparison of  $\theta$  angles of the Cu(bfp)<sub>2</sub><sup>+</sup> and Cu(dmp)<sub>2</sub><sup>+</sup> complexes confirms that the Cu(bfp)<sub>2</sub><sup>+</sup> cation distorts much less than the bis-dmp ion.

The bromide complex **3** has the least distorted geometry. It shows almost negligible rocking ( $\theta_x = 88.8^\circ$ ,  $\theta_y = 88.2^\circ$ ) and minor flattening ( $\theta_z = 86.7^\circ$ ) distortions. The largest rocking distortion is found in the hexafluorophosphate complex **2**, with  $\theta_y = 78.7^\circ$ . Overall, the rocking distortion is uncommonly large (7–10°) in the Cu(bfp)<sub>2</sub><sup>+</sup> cations surveyed here. The exceptions are complex **3** and one of the symmetrically independent molecules in **6**. The rocking distortion correlates with one of the two Cu–N bonds to the ligand being longer, as the rocking moves one bond toward the axial position of the trigonal pyramid (Table 2). The correlation is demonstrated in Figure 2, which shows the difference between the Cu–N bonds to increase with the rocking and wagging distortions.

As in the Cu(dmp)<sub>2</sub><sup>+</sup> compounds the copper atom is generally displaced from both phenanthroline planes in all the complexes, but the correlation with the rocking distortion is not as pronounced as for the Cu(dmp)<sub>2</sub><sup>+</sup> compounds. Whereas the copper displacement tends to increase when the

(18) (a) Zefirov, Yu. V.; Zorkii, P. M. *Rus. Chem. Rev.* **1989**, *58*, 421–440. (b) Zefirov, Yu. V.; Porai-Koshits, M. A. *Zh. Strukt. Khim.* **1979**, *21*, 150–155.

(19) Dobson, J. F.; Green, B. E.; Healy, P. C.; Kennard, C. H. L.; Pakawatchai, C.; White, A. H. *Aust. J. Chem.* **1984**, *37*, 649–659.

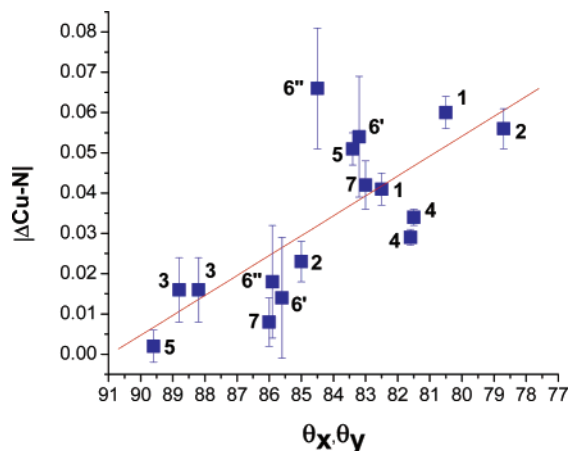


**Figure 2.** Correlation between the differences between the Cu–N distances ( $\Delta|Cu-N1-Cu-N2|$ ,  $\Delta|Cu-N4-Cu-N3|$ ) and the distortion parameters  $\theta_x$  and  $\theta_y$ . 6' and 6'' correspond to the two symmetrically independent molecules in the asymmetric unit of complex **6**.

rocking distortion is bigger, the largest displacement occurs for the tetrafluoroborate compound **1**, in which the rocking is second largest after complex **2**. The most noticeable exception is observed for the anthraquinone-2-sulfonate salt (**7**), in which the rocking distortion is  $7.0^\circ$ ; but the Cu displacement is insignificant.

Although, the  $\theta$  angles provide a good description of the deformation of the Cu coordination from the tetrahedral geometry and allow comparison of different cations, a single parameter to quantify the degree of distortion is desirable. For this purpose, we introduce the  $\zeta_{CD}$  function defined as:

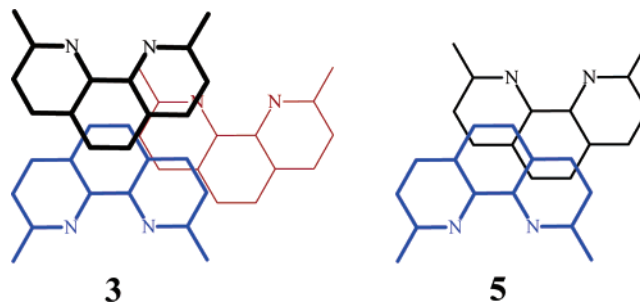
$$\zeta_{CD} = \frac{(90 + \theta_x)(90 + \theta_y)(90 + \theta_z)}{180^3}$$

where  $\theta_x$ ,  $\theta_y$ , and  $\theta_z$  are always  $\leq 90^\circ$  and the subscript CD stands for “combined distortion”. The  $\zeta_{CD}$  values are listed in Table 2, which shows the combined distortion to be largest for the cation in **4**, even though the wagging is most pronounced in **2**. The correlation between the  $\zeta_{CD}$  value and the triplet excited-state lifetime of the cation for the compounds **1–7** is discussed below.

Unlike the  $Cu(dmp)_2^+$  cation, the bis-bfp complexes do not form  $\pi-\pi$  stacks in the majority of the crystals studied. In just two of the salts weak  $\pi-\pi$  stacking interactions between bfp ligands are found (Scheme 1). In **3**, bfp ligands form infinite  $\pi-\pi$  stacks, with only limited overlap, the ligands being offset from each other, with plane-to-plane separations of 3.48 and 4.03 Å. The ligands are grouped into  $\pi-\pi$  dimers in **5**, with an interplanar distance of 3.52 Å, and overlap only slightly.

A different crystal packing is found in the 9,10-anthraquinone-2-sulfonate salts **6** and **7**. In **6**,  $AQSO_3^-$  anions form stacks along the crystallographic  $b$  axis, composed of center-of-symmetry related  $\pi-\pi$  dimers. The stacks are randomly broken by insertion of  $AQSO_3^-$  or  $BF_4^-$ . The plane of the interspersed anthraquinone-sulfonate is inclined by  $44^\circ$  to the adjacent component of the dimer. These dimers are flanked by two  $Cu(bfp)_2^+$  cations (Figure 3a). Although bfp and  $AQSO_3^-$  are parallel, they overlap only slightly

**Scheme 1**  $\pi-\pi$  Stacking Modes of the bfp Ligands in Crystals of **3** and **5**<sup>a</sup>



<sup>a</sup> Part of the infinite  $\pi-\pi$  stacks (bfp in blue is located between the other two) and a  $\pi-\pi$  dimer are shown for **3** and **5**, respectively. Fluorine atoms are omitted for clarity.

(Figure 3b). The shortest contact  $O1 \cdots C49'$  ( $1-x, 1-y, -z$ ) of 3.38 Å is between the carbonyl oxygen of the anthraquinone sulfonate and one of the bfp aromatic carbons. In the pure salt **7**, the  $AQSO_3^-$  anions form only centrosymmetric  $\pi-\pi$  dimers, separated from each other by  $Cu(bfp)^+$  cations. However, unlike in the mixed salt **6**, no  $\pi$  interactions are found between the cations and the anions, the bfp and  $AQSO_3^-$  planes being inclined to each other by  $62^\circ$  and  $81^\circ$  (Figure 3c). The closest contacts are  $O1 \cdots C7'$  ( $1-x, -y, -z$ ) 3.16 Å and  $C30 \cdots F7'$  3.14 Å. Therefore, the interactions between the cation and the anion are much weaker in complexes **6** and **7** than in  $[Cu(dmp)_2](AQSO_3)$ .<sup>13</sup> This has its important implications for the photoluminescence properties of the first two compounds.

**UV–Vis Absorption.** UV–Vis absorption (reflectance) and photoluminescence measurements were carried out on crystalline samples of all seven  $Cu(bfp)_2^+$  complexes.

The reflectance spectra of **1–7** are very similar (Figure 4) and show a low-energy absorption band centered at 467–474, with a shoulder at 542–558 nm (Table 3). Compared to bis-dmp  $Cu(I)$  systems, for which the bands shift by as much as  $\sim 40$  nm, no significant variation with the distortion around the copper is observed. Following Parker and Crosby<sup>20</sup> and Zgierski<sup>21</sup> both visible absorption bands are assigned to MLCT  $d_{xz,yz} \rightarrow \pi^*_{bfp}$  transitions from the highest occupied orbital. Only the higher energy transition ( $\sim 470$  nm) is symmetry-allowed for the ideal  $D_{2d}$  symmetry of the cation, and it has the largest intensity. The lower-energy band ( $\sim 550$  nm shoulder) appears in the solid-state spectrum due to symmetry lowering to  $C_1$ , which eliminates the symmetry selection rules. The near-UV bands appearing for all the compounds at 425–438 nm are due to the metal-to-ligand  $d_{xy} \rightarrow \pi^*_{bfp}$  transition, while the UV bands are assigned to the intraligand  $\pi_{bfp} \rightarrow \pi^*_{bfp}$  transitions.

**Emission Spectra and Lifetimes.** In the crystalline phase the  $Cu(bfp)_2^+$  complexes show strong orange-red emission. The emission is characterized by a very broad featureless spectra positioned in the 645–690 and 670–695 nm range at room and low (17 K) temperatures, respectively.

As is the case for the  $Cu(dmp)_2^+$  complexes and for a series of  $[Cu(NN)_2]^+$  type complexes with larger 2,9 sub-

(20) Parker, W. L.; Crosby, G. A. *J. Phys. Chem.* **1989**, *93*, 5692–5696.

(21) Zgierski, M. Z. *J. Chem. Phys.* **2003**, *118*, 4045–4051.

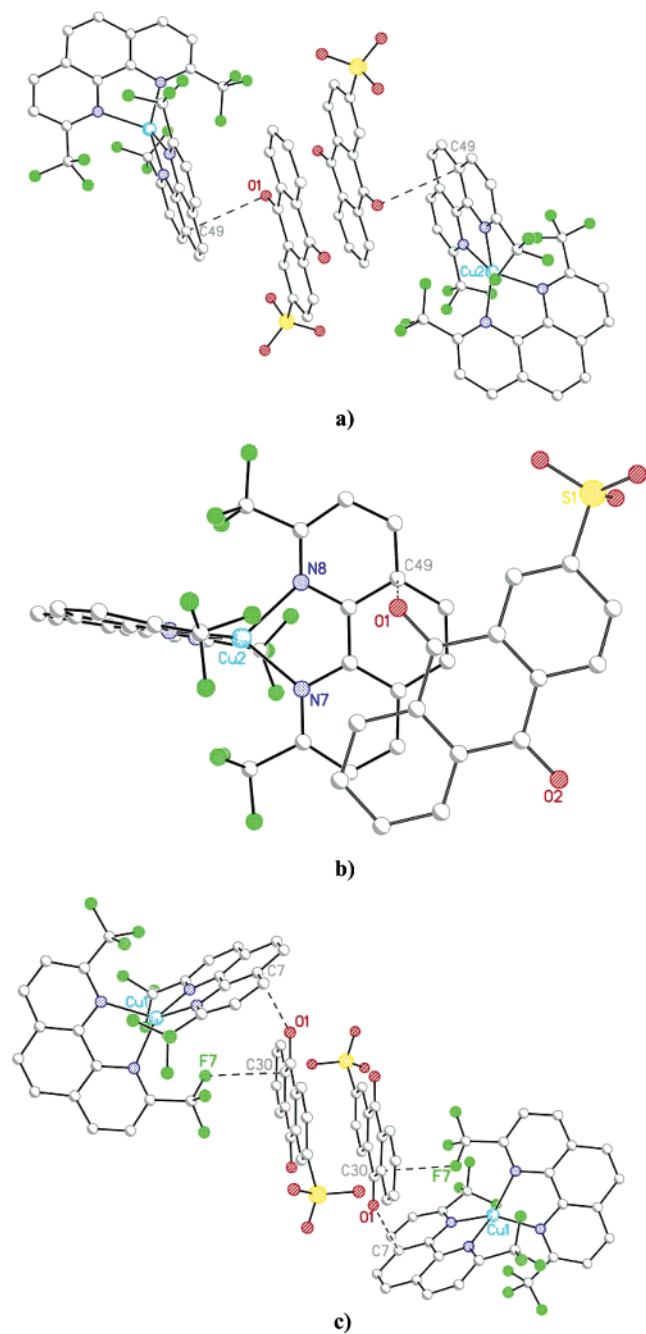


**Figure 3.** Intermolecular interactions between AQSO<sub>3</sub><sup>-</sup> anions and Cu(bfp)<sub>2</sub><sup>+</sup> cations in the crystals of complexes **6** (a and b) and **7** (c).

stituents,<sup>22</sup> the photoluminescence intensity weakens and the triplet excited-state lifetime increases when the temperature is lowered. On average the lifetime increases 2–3 times, while the emission maxima red-shift by 5–25 nm (100–580 cm<sup>-1</sup>). The behavior suggests the existence of two emissive excited states, possibly due to spin–orbit coupling, the higher energy one being thermally populated at room temperature.<sup>22,23</sup>

(22) Felder, D.; Nierengarten, J.-F.; Barigelletti, F.; Ventura, B.; Armaroli, N. *J. Am. Chem. Soc.* **2001**, *123*, 6291–6299.

(23) (a) Kirchoff, R. K.; Gamache, R. E.; Blaskie, M. W.; Del Paggio, A. A.; Lengel, R. K.; McMillin, D. R. *Inorg. Chem.* **1983**, *22*, 2380–2384. (b) Everly, R. M.; McMillin, D. R. *J. Phys. Chem.* **1991**, *95*, 9071–9075.

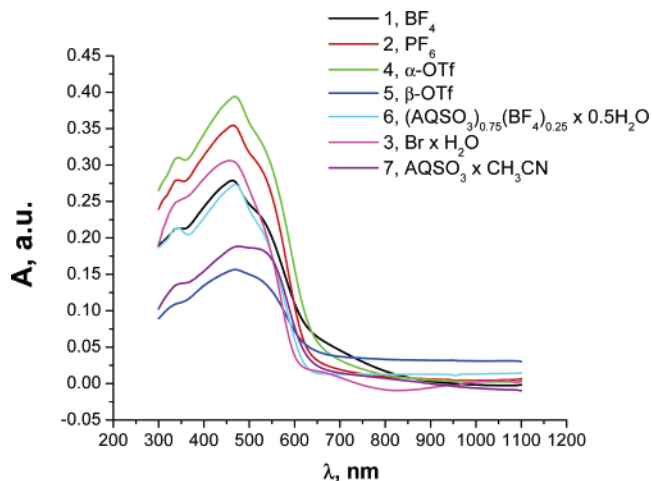


**Figure 4.** Room temperature solid-state absorption (reflectance) spectra from complexes **1**–**7**.

Comparison of the excited-state lifetimes of Cu(bfp)<sub>2</sub><sup>+</sup> and Cu(dmp)<sub>2</sub><sup>+</sup> cations shows that, in general, the substitution of hydrogen by fluorine increases the lifetime. However, the record established by the Cu(dmp)<sub>2</sub>(Tos) salt ( $\tau = 2.4 \mu\text{s}$  at 16K) is not exceeded. The largest <sup>3</sup>MLCT excited-state lifetime in the current series is 1.80(9)  $\mu\text{s}$  at 17 K measured for the BF<sub>4</sub> salt **1**.

#### Structural Distortion and Photophysical Properties.

The correlation between the overall distortion parameter ( $\zeta_{\text{CD}}$ ) and the excited-state lifetimes is remarkably strong. For all but one of the complexes, a linear relationship exists between increasing lifetime and decreasing distortion of the copper environment at both room and low temperature (Figure 5). Thus, the smaller the distortion of the Cu environment, the longer the excited-state lifetime. The exception is complex **1**. Although the distortion in [Cu(bfp)<sub>2</sub>]<sub>2</sub>BF<sub>4</sub> ( $\zeta_{\text{CD}} = 0.896$ ) (**1**) is as large as in **2** and **4** ( $\zeta_{\text{CD}} = 0.899$  for **2**, and  $\zeta_{\text{CD}} = 0.893$  for **4**, Table 2), its excited-state lifetime is considerably longer. This difference is even more pronounced at low temperature ( $\tau = 1.80(9) \mu\text{s}$ ), the lifetimes for **2** and **4** at 17 K being 1.00(5) and 0.83(4)  $\mu\text{s}$ , respectively. Clearly other effects such as less efficient intermolecular energy transfer due to packing differences can play a role in the solid state.

At both room temperature and 17 K the radiative lifetime  $\tau$  correlates with the wavelength of the emission, the lifetime being longer for a blue-shifted emission (Figure 6), in agreement with the energy-gap law for internal conversion.<sup>24</sup> Since the experiments have been performed with crystalline samples, it is now possible to correlate this behavior with the molecular geometry. The comparison shows that the S<sub>0</sub>–T<sub>1</sub> gap is smaller for the more distorted structures, which suggests that the variation of the geometry in the triplet excited state shows less variation than in the ground state.

Complexes **6** and **7** differ from the others studied here by having an electron-accepting counterion AQSO<sub>3</sub><sup>-</sup>. Previously, we reported<sup>13</sup> that the presence of this counterion in

(24) Turro, N. J. *Modern Molecular Photochemistry*; University Science Books: Sausalito, CA, 1978.

**Table 3.** Solid-State Absorption and Emission Data

	[Cu(bfp) <sub>2</sub> ] BF <sub>4</sub> <b>1</b>	[Cu(bfp) <sub>2</sub> ] PF <sub>6</sub> <b>2</b>	[Cu(bfp) <sub>2</sub> ] Br·H <sub>2</sub> O <b>3</b>	[Cu(bfp) <sub>2</sub> ] Tf α <b>4</b>	[Cu(bfp) <sub>2</sub> ] Tf β <b>5</b>	[Cu(bfp) <sub>2</sub> ] (AQSO <sub>3</sub> ) <sub>0.75</sub> (BF <sub>4</sub> ) <sub>0.25</sub> ·0.5H <sub>2</sub> O <b>6</b>	[Cu(bfp) <sub>2</sub> ] AQSO <sub>3</sub> ·CH <sub>3</sub> CN <b>7</b>
Solid-State Diffuse Reflectance Spectra							
RT, λ <sub>max</sub> , nm	335	337	335sh	338	331sh	339	335
	433sh	432sh	425sh	438sh	426sh	437sh	425sh
	467	468	473	473	468	474	470
	542sh	550sh	551sh	555sh	554sh	545sh	558sh
Solid-State Emission (λ <sub>exc</sub> = 500 nm)							
λ <sub>max</sub> (RT), nm	650	660	645	690	645	665	650
τ (RT), μs	0.61(3) <sup>a</sup>	0.41(2)	0.73(4)	0.40(2)	0.81(4)	0.52(3)	0.60(3)
λ <sub>max</sub> (17 K), nm	670	685	670	695	670	690	685
τ (17 K), μs	1.80(9)	1.00(5)	1.72(9)	0.83(4)	1.68(8)	1.36(7)	1.11(5)

<sup>a</sup> Standard deviations are estimated to be 5%.

the crystal with Cu(dmp)<sub>2</sub><sup>+</sup> cation results in total quenching of the phosphorescence for the complex [Cu(dmp)<sub>2</sub>]AQSO<sub>3</sub>·0.5H<sub>2</sub>O. However, the emission from crystals of **6** and **7** is readily detectable and is by no means less intense than for the other crystals. As mentioned above, in the crystals of both salts only a few relatively weak interactions are found between the bfp ligands and the AQSO<sub>3</sub><sup>-</sup> counterions, compared to a number of stronger interactions found in the corresponding bis-dmp complexes, indicating that crystal packing can play a crucial role in the phosphorescence quenching, in agreement with generally accepted concepts.<sup>25</sup>

## Conclusions

The Cu(I)(bfp)<sub>2</sub><sup>+</sup> cation in the different solids examined shows only moderate variation in geometric distortion of the Cu coordination environment in different crystallographic environments. The distortions around the copper metal are in general less pronounced (especially the flattening) than for the bis-dmp cation and do not markedly affect the absorption spectra. To examine the correlation between the ground-state geometry of Cu(bfp)<sub>2</sub><sup>+</sup> and its <sup>3</sup>MLCT excited-state lifetime, a geometric parameter (ζ<sub>CD</sub>) has been defined, which is a measure for the combined distortion of the metal coordination environment. With one exception, ζ<sub>CD</sub> correlates linearly with the observed phosphorescence lifetimes, the smaller the distortion from the ideal pseudo-tetrahedral geometry, the longer the lifetime. The complex [Cu(bfp)<sub>2</sub>]-BF<sub>4</sub>, which has the second largest rocking distortion but the longest lifetime of the complexes studied here, is an exception, indicating that other factors such as less efficient intermolecular energy transfer play a role.

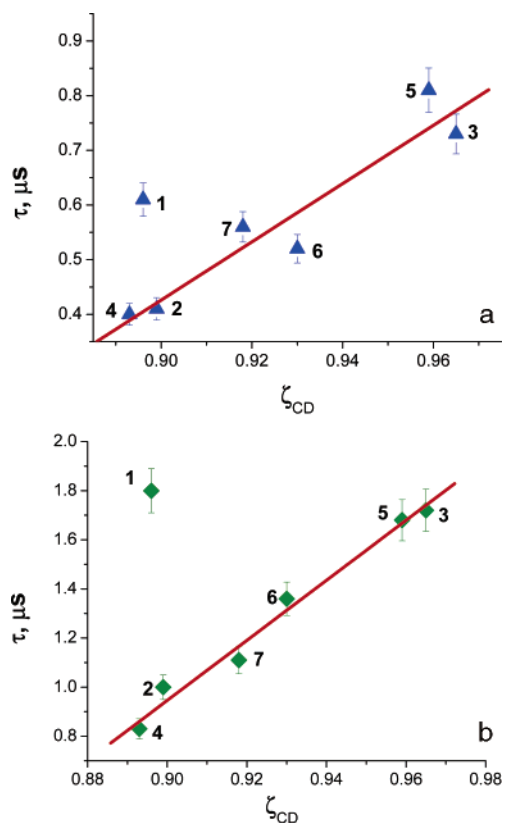


**Figure 5.** Correlation plots of the excited-state lifetimes (τ) vs the combined distortion values (ζ<sub>CD</sub>) at room (a) and 17 K (b) temperatures for compounds **1–7**. Error bars shown are with 5% margin. ζ<sub>CD</sub> = 1 corresponds to an undistorted structure.

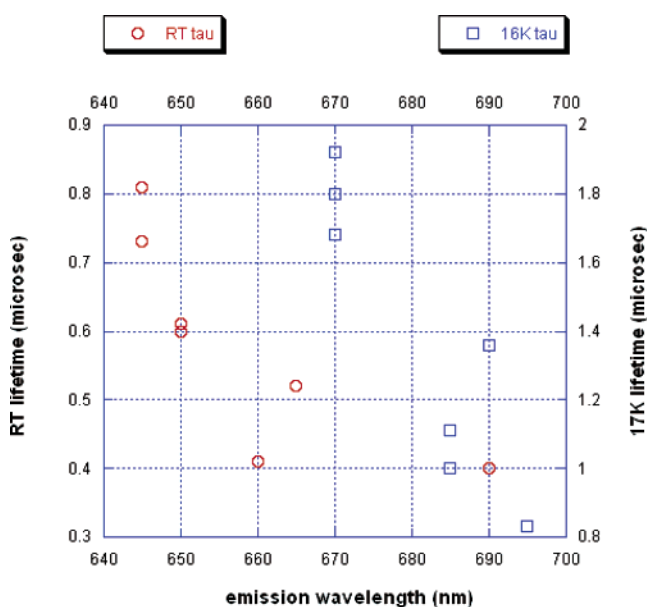


**Figure 6.** Correlation plots of the excited-state lifetime vs emission wavelength for **1–7** at RT and 17 K. Note the difference in scale for the RT (left) and the 17 K (right) lifetimes.

The emission wavelength of the triplet state tends to red-shift with decreasing lifetime and thus with increasing ground-state distortion. Determination of the excited-state geometries by time-resolved diffraction methods would provide further insight in the relation between structure and photophysical properties in this series of compounds.

---

(25) See, for example, Lower, S. K.; El Sayed, M. A. *Chem. Rev.* **1966**, *66*, 199–241.

**Acknowledgment.** Financial support of this work by the National Science Foundation (CHE9981864 and CHE0236317) is gratefully acknowledged.

**Supporting Information Available:** Tables of crystallographic information; X-ray crystallographic files in CIF format for the structures of **1–7**. This material is available free of charge via the Internet at <http://pubs.acs.org>.

IC049638S